

NISTIR 5058 (Revised)

Noncontact Measurement of the Exit Temperature of Sheet Metal in an Operating Rolling Mill

Arnold Kahn
Louis C. Phillips
Stephen R. Schaps
George A. Alers

NISTIR 5058 (Revised)

Noncontact Measurement of the Exit Temperature of Sheet Metal in an Operating Rolling Mill

Arnold Kahn*
Louis C. Phillips*
Stephen R. Schaps
George A. Alers

Materials Reliability Division
Materials Science and Engineering Laboratory
National Institute of Standards and Technology
Boulder, Colorado 80303-3328

*Metallurgy Division
Materials Science and Engineering Laboratory
National Institute of Standards and Technology
Gaithersburg, Maryland 20899-0001

April 1998



U.S. DEPARTMENT OF COMMERCE, William M. Daley, Secretary
TECHNOLOGY ADMINISTRATION, Gary R. Bachula, Acting Under Secretary for Technology
NATIONAL INSTITUTE OF STANDARDS AND TECHNOLOGY, Raymond G. Kammer, Director

NONCONTACT MEASUREMENT OF THE EXIT TEMPERATURE OF SHEET METAL IN AN OPERATING ROLLING MILL

Arnold Kahn and Louis C. Phillips

National Institute of Standards and Technology, Gaithersburg, MD

Stephen R. Schaps and George A. Alers

National Institute of Standards and Technology, Boulder, CO

An accurate knowledge of the temperature of sheet aluminum as it moves out of the last stand of the hot mill is very important to the production of a uniform product that meets the customer's specifications. Because the emissivity of the sheet is poorly defined and the sheet is covered with boiling coolants at the exit stand, infrared techniques for monitoring the temperature are subject to large errors. This report describes the development of a noncontacting thermometer based on eddy currents that measures the electrical resistivity of the aluminum alloy while it is being rolled. By combining off-line calibration data with other quantities measured on-line, the resistivity measurement can be converted into the temperature of the sheet in real time. Data collected during on-line tests of a prototype system at a commercial hot mill indicated a 3σ measurement uncertainty of $\pm 11^\circ\text{C}$ ($\pm 20^\circ\text{F}$) in the exit temperature, neglecting any systematic errors arising from the calibration techniques used. The primary source of this uncertainty was introduced by a contacting thermocouple at the entrance to the hot mill where the alloy slab being rolled was calibrated to make it act as its own resistance thermometer. Reasonable improvements in this temperature measurement can reduce this uncertainty to $\pm 8^\circ\text{C}$ ($\pm 14^\circ\text{F}$) and even to $\pm 4^\circ\text{C}$ ($\pm 7^\circ\text{F}$) if the resistivity measurement techniques were optimized for the mill conditions.

Keywords: aluminum sheet; eddy current; process monitoring; resistivity; temperature

1. INTRODUCTION

During the extrusion or rolling of aluminum products, the quality of the final product depends critically on an accurate knowledge of the temperature as the metal leaves the last processing step. This is particularly true for the rolling of sheet aluminum where such commercial properties as the formability, the surface appearance and the mechanical strength of an entire coil are strongly influenced by the temperature of the sheet as it leaves the final rolling stand and is coiled up for cooling and shipment. Unfortunately, temperature measurement at this location is difficult because the sheet is moving at high speed, its surface is covered with coolants, and its location can wander about the pass line. Modern infrared sensors are hampered by the variations in emissivity that accompany the naturally shiny surface of aluminum and by the low absolute temperatures at which aluminum forming is performed. Thus, they may not be the technology of choice at the mill exit. Eddy-current temperature sensors that are based on the temperature dependence of the electrical resistivity of metals can be made into noncontact devices and,

therefore, could operate on a moving sheet. Such devices are commercially available for operation near room temperature, but the small clearance they require between the sensor head and the material being measured prevents their immediate application to the exit stand of an operating rolling mill. This paper discusses a high-temperature eddy-current probe that tolerates several centimeters of clearance [1] and has been demonstrated to be capable of operation in a commercial rolling mill.

The program described in this report was undertaken as a Cooperative Research And Development Agreement (CRADA) between the Aluminum Association and NIST to demonstrate the feasibility of using an eddy-current measurement of the resistivity of moving sheet to deduce its temperature under the following conditions:

1. The air gap between the sensor and the sheet should be approximately 30 cm (12 in) — a distance commonly used by the X-ray thickness gages in most mills.
2. The accuracy of the measurement of temperature by the sensor should not be sensitive to the speed of the sheet as it passes under the sensor.
3. The accuracy should not be sensitive to fluctuations in the nominal position of the sheet compared with respect to the pass line of the rolling mill.
4. The accuracy should be independent of lubricants and cooling liquids on the surface of the sheet at the exit end of the mill.

Once these requirements were met in laboratory tests, a mill-worthy, first-prototype measurement system was assembled so that on-line operation could be tested at a commercial rolling mill. This report summarizes the results of these on-line tests. It is concluded that the eddy current approach to noncontact measurement of temperature can be applied to the exit stand of an operating rolling mill and that it can yield 3σ uncertainties of ± 8 to 11°C , which is not far from the ± 6 to 12°C experienced with contacting thermocouples [2] and is comparable with the ± 8 to 16°C observed with modern infrared radiation thermometers when used under mill conditions on a wide variety of alloys [2].

2. NONCONTACT TEMPERATURE MEASUREMENT BY EDDY CURRENT TECHNIQUES

2.1 Principles of Electrical Resistance Thermometry

The fact that the electrical resistivity of metals depends upon the temperature allows a measurement of resistivity to be used as a thermometer. In fact, the platinum-resistance thermometer provides a primary standard for temperature measurement and is often used to calibrate thermocouples and other types of thermometers. In the present case, the aluminum itself provides the resistive element. The only problem is the development of a technique for measuring the electrical resistance without making physical contact with the material. By employing

alternating currents and theoretical models for electromagnetic induction across large air gaps, the noncontact requirement demanded by this application can be met and the performance of practical sensor coils can be predicted. For aluminum and its alloys, the relationship between resistivity and temperature is taken to be

$$\rho(T) = \rho_a(T) + \Delta\rho, \quad (1)$$

where $\rho(T)$ is the resistivity of the aluminum sheet at temperature T , $\rho_a(T)$ is the known resistivity of pure aluminum at temperature T and $\Delta\rho$ is a resistivity increment introduced by the alloying elements in the particular aluminum alloy being rolled. The fact that $\Delta\rho$ is a simple additive constant is known as Matthiessen's rule and is considered to be an adequate description for commercial aluminum alloys [3]. Values for the temperature dependence of the resistivity $\rho_a(T)$ of pure aluminum can be found in the literature [4,5,6,7] and are listed in Appendix A. The following formula describes these values:

$$\rho_a(T) = 2.428 + 0.0104T + 2.91 \times 10^{-6}T^2, \quad (2)$$

where T is in degrees Celsius. This is an essentially linear function with a small quadratic term to account for small deviations from linearity at high temperature. The values of the coefficients were chosen to minimize the deviations from the values found in the literature. Figure B-1 in the Appendix shows that these deviations can be as much as $\pm 6^\circ\text{C}$ which represents the uncertainty relative to the absolute thermodynamic temperature. Equation (2) will be used for the purposes of assessing the precision with which a temperature can be deduced from resistivity measurements but it must be understood that the absolute thermodynamic temperatures deduced from eq (2) may be in error by $\pm 6^\circ\text{C}$. Reducing this error in absolute temperature will require careful reevaluation of the temperature dependence of the resistivity of pure aluminum using modern laboratory techniques. In order to deduce the temperature from a measured resistivity, we combine eq (1) and eq (2) and rearrange terms to obtain the quadratic equation

$$T^2 + 3574T + 3.436 \times 10^5[\Delta\rho - \rho(T) + 2.428] = 0. \quad (3)$$

Its solution is

$$T = 586.2 \{[\rho(T) - \Delta\rho] + 6.864\}^{1/2} - 1787, \quad (4)$$

where $\rho(T)$ is the measured resistivity in $\mu\Omega\cdot\text{cm}$ of the sheet aluminum at the desired point in the rolling process. The uncertainty in the temperature measurement, δT , can be related to the uncertainty in the resistivity measurement by differentiating eq (4) to obtain

$$\delta T = 293.1 \{[\rho(T) - \Delta\rho] + 6.864\}^{-1/2} \delta\rho. \quad (5)$$

For our purposes, which involve resistivities in the range of 7 to 11 $\mu\Omega\cdot\text{cm}$, this relationship can be adequately approximated by

$$\delta T = 77\delta\rho. \quad (6)$$

This equation relates the uncertainty in temperature in kelvins to the uncertainty in a resistivity measurement in $\mu\Omega\cdot\text{cm}$.

The following two sections of this report discuss the details of the design and use of eddy-current probes that operate with a large air gap above the fast-moving, thin aluminum sheet at the exit end of the mill and that operate with a small air gap above the thick aluminum slab entering the mill, where the material is momentarily at rest. In both cases, the probes were constructed of materials capable of withstanding high temperatures and the hostile mechanical and chemical environment of an operating aluminum rolling mill.

2.2 Description of the Exit Probe

Because of the requirement for measuring the resistivity of rapidly moving sheet metal at the exit stand of a rolling mill, an eddy-current technique that can operate at air gaps of 10 to 30 cm was demanded. The final design employed a through-transmission method that used a pair of coils one mounted above and one below the pass line of the mill. The electrical quantity measured was the electromagnetic coupling between these two coils as if they were the primary and secondary windings of a transformer. When the sheet was in place between the coils, it acted as an attenuator or a shield between the primary and secondary coils to make the secondary's output signal smaller by an amount determined by the thickness and resistivity of the aluminum sheet. The fact that the sheet may be moving and covered with nonconducting liquids has a negligible effect on the electromagnetic coupling. Furthermore, if the sheet is approximately midway between the coils, its exact location has little or no effect on the coupling efficiency. Thus, all the requirements listed in the introduction are satisfied.

Figure 1 shows a schematic diagram of a hot mill with the aluminum entering as a thick slab on the lower left and exiting as thin coiled sheet on the lower right. Just after the final rolling reduction, a commercial X-ray thickness gage measures the exit thickness of the sheet and adjacent to that, the two eddy-current coils are mounted above and below the pass line. The figure also shows a block diagram of the electronic circuitry needed to measure resistivity at both the entrance and exit ends of the mill. It also shows a personal computer where the data were analyzed and converted into values of temperature by special software developed for the on-line tests. This computer also responded to signals from the rolling mill, which allowed it to operate relays for activating either the entry or exit probes at separate times.

To demonstrate feasibility, a commercial impedance analyzer instrument was used to take all the electrical measurements. It was set up to measure the transfer impedance of a pair of coils over a wide range of frequencies.

During operation of the exit probe, an alternating current from the impedance analyzer excited the primary eddy-current coil in series with a power amplifier and a precision resistor. The primary coil was mounted above the sheet of aluminum. By measuring the voltage across the precision resistor, the impedance analyzer sensed the magnitude and phase of the current through the primary coil. The voltage output of the secondary coil, mounted on the opposite side of the sheet, allowed the instrument to determine a unitless gain parameter G and a phase parameter θ at a series of frequencies. Using these values of G and θ , the instrument executed a program to output the effective impedance of the transformer circuit formed by the two coils with the

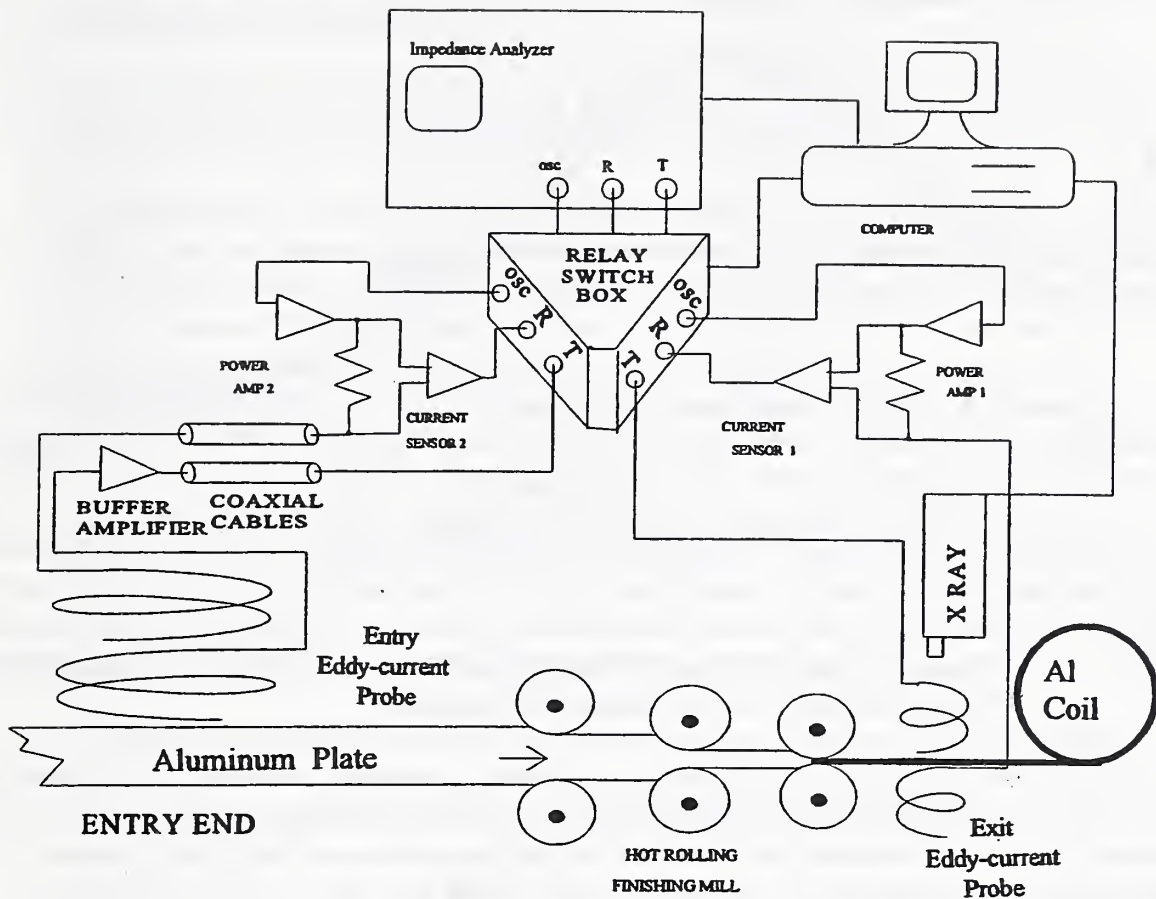


Figure 1. Block diagram of the eddy-current thermometer developed by NIST for measuring the exit temperature of aluminum alloy sheet at the exit end of a hot rolling mill.

aluminum sheet in between. This impedance is a complex number with real and imaginary parts whose numerical values depend on the geometrical and electrical properties of the coils and the resistivity and thickness of the aluminum sheet. When the aluminum sheet is absent, the instrument outputs impedance values that contain only the geometrical and coil properties. From the ratio of the output impedances with and without the aluminum, normalized impedances dominated by the of aluminum can be obtained. These normalized impedances can also be calculated from electromagnetic theory for specific geometrical configurations of coils and sheets, so mathematical relationships between all the parameters can be used as aids in analyzing the measurements.

Figure 2 shows an example of how the normalized ratio of the real impedances of the two coil "transformer" varied as the frequency used in the impedance measurements was swept

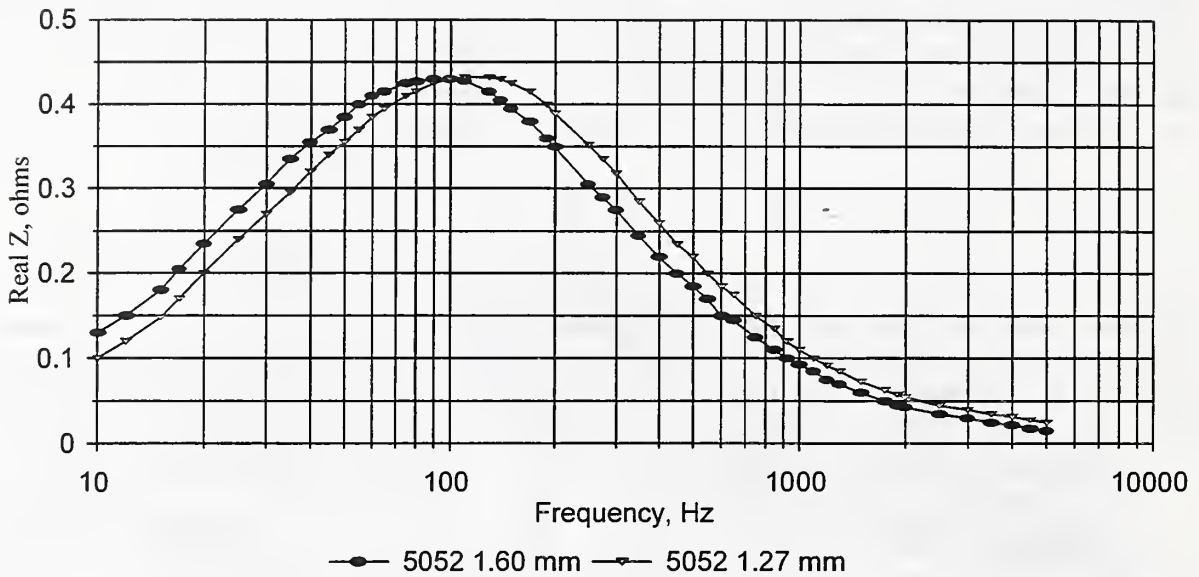


Figure 2. Variation of the real part of the transfer impedance between the two coils of the exit eddy-current probe as a function of frequency.

from 10 Hz to 10,000 Hz for the case of two thicknesses of 5052 aluminum sheets. The prominent feature is a maximum in the normalized real impedance at a particular frequency. A theoretical analysis shows that the frequency f_0 at which the maximum occurs is a simple function of thickness d of the sheet and its resistivity $\rho(T)$ at the temperature of measurement. Specifically, the relationship can be written

$$\rho(T) = K \cdot f_0 \cdot d, \quad (7)$$

where K is a geometrical constant determined by the geometry and electrical properties of the coils used at a particular mill, f_0 is the frequency at which a maximum in the transfer impedance between the two measurement coils is observed, and d is the thickness of the sheet at the exit end of the mill as measured by an x-ray thickness gage located at the exit end.

During the past several years, various tests were carried out at the NIST laboratories in Gaithersburg, Maryland, and at two commercial rolling mills in North America to test the features of the two-coil concept for measuring $\rho(T)$. The results can be summarized by the following statements.

1. The motion of the sheet above and below the pass line by a few centimeters introduced errors of less than 0.1% in the resistivity.

2. The presence of fluids, steam, and bubbles on or near the sheet surface does not appear to introduce any variations in the eddy-current coil outputs, so their effect on $\rho(T)$ measurements is insignificant.
3. Tests of the insensitivity to the speed of the sheet up to 4 m/s (700 ft/min) do not expose any errors that could be attributed to the motion of the sheet.
4. Tests performed with different distances between the eddy current coils and the surface of the sheet show that larger signal-to-noise ratios would accompany smaller distances, and some improvements in the accuracy of the temperature measurement should be obtained if the air gap is reduced to 7.5 cm (3 in).

The 3σ uncertainty in f_0 and in d were estimated from observations of the fluctuations in the output of the instrumentation used to measure these two quantities. (That is, the 3σ uncertainty was taken from the statistical relationship that 99% of the readings will fall within a 3σ range if the errors are random and follow a Gaussian distribution.) The uncertainty in K has been estimated from calibration measurements made on a collection of aluminum sheet samples with various compositions and thicknesses. Following improvements in the system introduced during the spring of 1995 and used in the rolling mill tests in the fall of 1995, the 3σ uncertainties in the three terms of eq (7) are $\delta K/K = 0.4\%$, $\delta f_0/f_0 = 0.3\%$, and $\delta d/d = 0.3\%$.

These are random uncertainties and do not account for any systematic uncertainties. When combined by the "root-sum-of-squares" method, these uncertainties yield the result that the 3σ uncertainty in the measured, on-line resistivity of the sheet at the exit to the mill is

$$\delta\rho(T)/\rho(T) = \pm 0.6\%. \quad (8)$$

This result is insufficient for calculating the uncertainty in the temperature because the temperature is deduced from the difference between the measured, total resistivity and the alloy contribution, $\Delta\rho$ (see eq (1)). Thus, the total temperature uncertainty is the square root of the sum of the squares of the uncertainties in the measured resistivity at the exit end of the mill and the alloy contribution. Expressed in terms of eq (6)

$$\delta T = 77 [\delta\rho(T)^2 + (\delta\Delta\rho)^2]^{1/2}, \quad (9)$$

where $\delta\rho(T)$ is 0.6% of $\rho(T)$ and $\delta\Delta\rho$ is the 3σ uncertainty in the alloy contribution. Since $\rho(T)$ is approximately $9 \mu\Omega\cdot\text{cm}$ over the temperature range of interest, $\delta\rho(T)$ is $0.054 \mu\Omega\cdot\text{cm}$. This would lead to a 3σ uncertainty in the exit temperature of only $\pm 4^\circ\text{C}$ if the alloy contribution, $\Delta\rho$, were known exactly and the coefficients in eq (2) are not changed by future calibration measurements.

2.3 Estimation of $\Delta\rho$

For simplicity of operation, it would be best to take $\Delta\rho$ from a look-up table prepared from laboratory measurements of the resistivity of a particular alloy. The uncertainty introduced by this

procedure (the value of $\delta\Delta\rho$) would simply be the 3σ uncertainty observed in measurements of the resistivity of a large number of samples of the same alloy at room temperature.

Laboratory tests on a set of 20 samples of 3004 alloy were made in 1992 with the result that a 3σ uncertainty in resistivity of $0.18 \mu\Omega\cdot\text{cm}$ was observed. The temperature uncertainty resulting from simply using this nominal value for $\Delta\rho$ for this alloy would then follow from eq (9) to be

$$\delta T = 77 \{ [\delta\rho(T)]^2 + [\delta\Delta\rho]^2 \}^{1/2} = 77 [(0.054)^2 + (0.18)^2]^{1/2} = \pm 15^\circ\text{C}, \quad (10)$$

which is considered to be unacceptable inaccuracy for the exit temperature.

In 1993, 50 samples of a 5052 alloy were measured by the exit eddy-current probe at room temperature. The results for the 3σ uncertainty in the alloy contribution, $\delta\Delta\rho$, was $\pm 0.113 \mu\Omega\cdot\text{cm}$. From eq (9), this corresponds to a 3σ uncertainty in the temperature for the combined exit and entrance eddy current probes of $\pm 10^\circ\text{C}$.

During the most recent (fall of 1995) tests at the commercial hot mill, room-temperature resistivities of samples cut from the ends of 115 hot slabs of various alloys were measured with a commercial conductivity tester. The results of these tests are presented in Table 1.

The largest standard deviation, $0.051 \mu\Omega\cdot\text{cm}$, is for alloy 5005, for which there are 17 examples. This standard deviation would correspond to a 3σ uncertainty of $0.153 \mu\Omega\cdot\text{cm}$ and would lead to a 3σ uncertainty of $\pm 13^\circ\text{C}$ in the exit temperature. By combining the results on the 3003 and

Table 1. Results from the commercial conductivity tester.

Alloy	No. of slabs	$\rho(20)$ ($\mu\Omega\cdot\text{cm}$)	$\Delta\rho$	Standard deviation
1145	14	2.748	0.111	0.014
110	10	2.821	0.184	0.007
5005	20	3.308	0.671	0.051
3003	28	3.755	1.118	0.008
3105	17	3.777	1.140	0.015
3005	6	4.189	1.552	0.005
5052	5	4.638	2.001	0.004
5154	4	4.950	2.313	0.005
5086	11	5.467	2.83	0.008

3105 alloys, which have nearly identical values of $\rho(20)$, we obtain a data set containing 45 examples, which allows a more reliable statistical analysis. In this case, the mean value of $\rho(20)$ is $3.763 \mu\Omega\cdot\text{cm}$, with a 3σ uncertainty of $\pm 0.128 \mu\Omega\cdot\text{cm}$. This would yield an overall systematic uncertainty of $\pm 11^\circ\text{C}$.

These direct measurements of the alloy contribution, $\Delta\rho$, for four alloy systems would indicate that the look-up table approach to determining $\Delta\rho$ would yield temperature inaccuracies for the exit temperature ranging from $\pm 10^\circ\text{C}$ to $\pm 14^\circ\text{C}$. This is far from the ultimate goal of $\pm 5^\circ\text{C}$ for the inaccuracy of the exit temperature, so a better procedure needs to be developed.

2.4 Measuring $\Delta\rho$ Directly with an Eddy-Current Probe at the Entrance

The entrance eddy-current probe has been designed to measure the resistivity of the hot slab as it sits to have its leading edge trimmed before entering the hot finishing mill where it is rolled into a thin sheet and coiled. Since the slab temperature is measured with a contact thermocouple at the same time, it is possible to calculate the resistivity of pure aluminum at that temperature from eq (2) and then calculate $\Delta\rho$ from eq (1). The resulting $\Delta\rho$ value, when combined with the electrical measurements at the exit probe, enables the sheet temperature at the exit end of the mill to be deduced with less uncertainty than that obtainable with a look-up table.

In the exit probe described above, the aluminum sheet lies between widely spaced primary and secondary coils. In the entry probe, the aluminum is positioned beside primary and secondary coils which are wound concentrically onto a single coil form. In both cases, the instrumentation measures the transfer impedance between the two coils. As indicated in Figure 1, the electrical connections to the primary and secondary coils are similar for both probes. A computer-controlled relay switches the oscillator and input channels of the impedance analyzer from one probe to the other for separating measurements at the entrance and exit ends of the mill when it is appropriate. The entry probe differs from the exit probe in the geometry of the coils, in the algorithm used for data analysis, and in the frequency range over which the instrumentation scans each probe. Unlike the exit probe, the entry probe is not sensitive to sheet thickness, but is sensitive to the air gap distance between the probe and the slab surface. Also, the exit probe measures the temperature of thin moving sheets while the entry probe measures $\Delta\rho$ on stationary thick slabs.

The entry probe was constructed of materials that could withstand repeated high temperature contacts with objects near 600°C (1100°F). It consists of a pair of pancake coils wound in spiral grooves on opposite faces of a square ceramic coil form 6.35 mm (0.25 in) thick by 102 mm (4 in) on a side. These two coils form the primary and secondary windings of a transformer whose coupling is very sensitive to the proximity of any conducting plate. A Teflon frame surrounding the coil form provides mechanical protection and three brass 'feet' support the Teflon frame when it rests on the hot aluminum slab. A small air gap between the probe and the aluminum slab is easy to achieve by simply allowing the probe to rest on the slab. An exactly reproducible dimension for this air gap could not be assured because the surface of the aluminum slab was seldom perfectly flat. In the rolling mill tests, the brass and ceramic coil frame was attached to a teflon mounting bracket on a hand-operated, steel lever-arm that allowed the probe to be lowered

onto the aluminum slab. When the probe rested on the aluminum slab, its frame floated free of the lever-arm mechanism with 2 inches of vertical movement and ½ inch of horizontal movement available.

During a production run at the mill, each rough-rolled aluminum slab was stopped to have its leading edge trimmed square and to have its temperature measured for entry into the hot finishing mill. At this time, the entry eddy-current probe was lowered with a hand-operated lever arm onto the slab and a small lift-off was established by the brass feet. Simultaneously, a hand-held, commercial thermocouple sensor was placed in contact with the slab less than 100 mm (4 in) from the center of the eddy-current probe and a measured reference temperature was recorded. The impedance analyzer then measured and recorded the transfer impedance of the two coils in the probe head in the same manner as was used for the exit probe measurements except that the frequency range over which the measurements were made extended from 1 kHz to 5 kHz. This frequency range was chosen to ensure that the electromagnetic skin depth was always small compared to the thickness of the slab. The data acquisition process itself consisted of automatically recording into the computer memory the results of averaging together 32 measurements of primary and secondary voltages at each of 20 frequencies. This entire process took less than 10 seconds and resulted in values for the magnitude, phase, and real and imaginary parts of the transformer impedance, as well as a series of temperature measurements while all the parts came to thermal equilibrium with the slab. On many occasions, the thermometer did not approach a constant reading as would be expected for a good thermal contact between the slab and the thermocouple. This occurred on 18 of the 137 slabs tested and the results of these tests were not used in subsequent analysis. After the electrical and temperature measurements had been recorded, the eddy-current probe was raised and the electrical measurements were repeated with the probe in air. This open-circuit measurement was used to normalize the data in a manner similar to the procedure used on the exit probe. This normalization of the impedance removes many electronic artifacts. Table 2 summarizes the results of using the entrance eddy-current probe on 137 coils processed by the rolling mill.

Table 2. Entrance eddy-current probe test results.

No. of coils	Results obtained
4	No measurement of either $\Delta\rho$ or $\rho(T)$
16	Referee thermocouple inoperative
18	Unreliable thermal contact of referee
40	Unreliable performance of eddy-current probe
59	Acceptable measurements of both $\rho(T)$ and $\Delta\rho$
137	Total coils processed (10 alloy types)

For calibrating the eddy-current entry probe for the conditions present at the Alumax mill, the trimmed ends of each slab measured by the probe were quenched and collected so that direct measurements of $\Delta\rho$ could be accumulated. These measurements were made with a commercial conductivity tester at the ambient temperature of the mill (often as high as 104°F) and corrected to 0°C by eq (2). Given values of $\Delta\rho$ and the temperature of the slab as measured by the contacting thermocouple, a value for the resistivity of the slab at the thermocouple temperature could be calculated from eqs (1) and (2). A table listing all 59 measurements of $\Delta\rho$ (Column 4) along with the temperatures read from the contacting thermocouple (Column 5) for each slab is given in Appendix A. Column 9 of this table lists the resistivity values calculated from these data through the use of eqs (1) and (2). Columns 6 and 7 list the phase and magnitude, respectively, of the impedance measured by the impedance analyzer on the hot slabs whose temperatures are listed in Column 5.

Calibration of the entrance eddy current probe under the rolling mill conditions consisted of using all of these 59 data points to establish most probable values for coefficients in a semi-empirical equation that relates the measured impedance values to the resistivity. The equation used is based on electromagnetic theory as well as on laboratory experiments that demonstrate that a linear relationship between impedance and resistivity is quite adequate to describe the data over the range of resistivities encountered in these tests. An important consideration in establishing the relationship between the impedance of a contacting eddy-current probe and the resistivity of the metal under it is how to remove variations in impedance caused by the air gap or lift-off between the eddy current sensor and the metal surface. In the present case of a hot slab, several methods were examined. All of them used the fact that the real and imaginary parts of the impedance represent two independent quantities which can be manipulated mathematically to give two separate quantities—the resistivity and the lift-off. Analysis of the data obtained during the mill tests showed that, for the range of conditions encountered, the magnitude and phase of the current in the secondary coil could both be expressed as linear functions of the resistivity and lift-off. By plotting the magnitude, M , and the phase, P , as a function of the resistivity deduced from the temperature and $\Delta\rho$ measurements, a linear regression analysis leads to the two empirical, linear equations

$$M = [\alpha\epsilon + 0.36045] + 0.0071228\rho, \quad (11)$$

$$P = [\beta\epsilon + 1.40895] - 0.006210\rho, \quad (12)$$

that best describe all of the data. Here, the bracketed terms are intercepts that include the coefficients α and β , which are constants that describe the sensitivity to the lift-off value, ϵ , present for each measurement. By rearranging terms in eqs (11) and (12), we can form expressions for the deviation of each data point from the linear regression line. These are:

$$\text{deviation in magnitude: } M - 0.0071228\rho - 0.36045 = \alpha\epsilon; \quad (13)$$

$$\text{deviation in phase: } P + 0.00621\rho - 1.40895 = \beta\epsilon. \quad (14)$$

The ratio of these two equations is an expression that is independent of ϵ and which can be used to determine the ratio α/β by determining the slope of the line formed by plotting the left hand

side of eq (13) versus the left hand side of eq (14). This analysis yielded $\alpha/\beta = 0.928$ which leads to the calibration equation that is independent of lift-off

$$\rho = 72.44M - 78.06P + 83.872, \quad (15)$$

for the conditions at the rolling mill where the tests were performed. This equation can now be used to determine the resistivity, ρ , from any set of measurements of the magnitude, M , and the phase, P , of the transfer impedance of the entrance eddy current probe at the rolling mill.

In order to access the accuracy that can be expected from the use of eq (15), we invert the analysis procedure by treating the 59 acceptable measurements of $\rho(T)$ and T listed in Appendix A as the results of a second series of 59 slab measurements. The measurements of the temperature of the slab by the contact thermocouple (Column 5) along with the associated magnitude and phase of the impedance (Columns 6 and 7) were inserted into eq (15) to yield a value for $\rho(T)$. This value is listed in Column 8 in Appendix A. Inserting the temperature (Column 5) into eq (2) yields the resistivity of pure aluminum at the temperature, T . Forming the difference between $\rho(T)$ and the resistivity of pure aluminum yields a value of $\Delta\rho$ that would be the results of the "second series" of tests. A comparison of these "second test" values of $\Delta\rho$ with the values of $\Delta\rho$ directly measured on the cut ends of the slabs (Column 4) provides a measure of the accuracy obtainable from the application of the calibration equation, eq (15). Figure 3 plots the values of $\Delta\rho$ deduced from measurements of impedance and temperature on the hot slab against the measurements of $\Delta\rho$ made at room temperature on the ends cut from the same slab.

All 59 acceptable measurements made at the mill are represented in Figure 3. The scatter of the individual data points around the line with a unit slope indicates the total uncertainty in $\Delta\rho$ to be expected from deducing $\Delta\rho$ from the semi-empirical equation, the temperature measurement and the impedance measurements.

A more informative way to present these data is to plot the deviations of each measurement from the line of unit slope that would represent a perfect agreement. This graph is shown in Figure 4(a). Here, it would appear that 97% of the data lie in the interval $\pm 0.15 \mu\Omega\cdot\text{cm}$. If the data were distributed in a Gaussian manner, the 3σ uncertainty would be $\pm 0.15 \mu\Omega\cdot\text{cm}$ for the entrance probe and the overall uncertainty of the exit temperature would be $\pm 13^\circ\text{C}$. It is noteworthy that each alloy type is represented by a cluster of points whose mean value appears to have a systematic deviation from the line of unit slope. This could be interpreted as a sensitive test of the accuracy of Matthiessen's rule. If one defines a small correction factor to be applied to Matthiessen's rule for a given alloy, the systematic deviations can be minimized and greater apparent accuracy achieved. Table 3 lists the corrections to be applied to each of the alloys tested at the rolling mill. A graph of the deviations after correcting Matthiessen's rule is shown in Fig. 4(b). Here, 97 percent of all the data lies in the interval of $\pm 0.09 \mu\Omega\cdot\text{cm}$ which would lead to a 3σ temperature uncertainty of $\pm 8^\circ\text{C}$ in the exit temperature. In order to determine if this modification of Matthiessen's rule is correct and if the reduction in scatter in the data is justified, it will be necessary to test many samples of many alloys. Such an extensive program is best

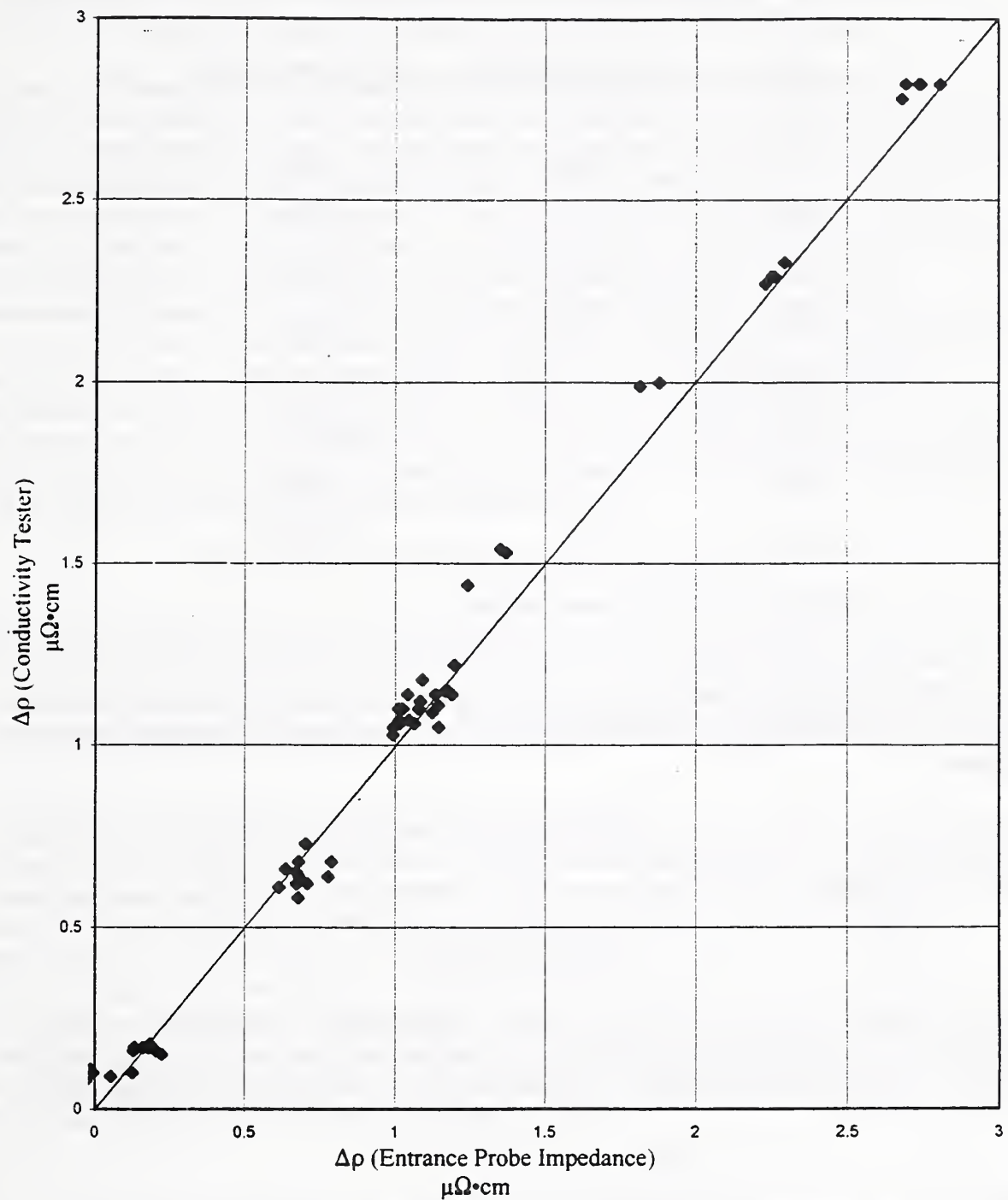


Figure 3. Comparison of the alloy contribution to resistivity, $\Delta\rho$, measured at room temperature by the commercial conductivity tester on ends cut from the hot slabs with values of $\Delta\rho$ deduced from a semi-empirical equation relating resistivity to the electrical impedance of the entrance eddy-current probe and the resistivity of pure aluminum at the temperature measured by the contacting thermocouple.

Table 3. Corrections to $\Delta\rho$ for the alloys tested at mill.

Alloy	Ave. $\Delta\rho$ ($\mu\Omega\cdot\text{cm}$)	Correction ($\mu\Omega\cdot\text{cm}$)
1145	0.112	+0.0611
110	0.185	+0.0169
5005	0.672	-0.0844
3003	1.112	+0.0150
3105	1.141	-0.0155
3005	1.553	+0.0940*
5052	2.003	+0.120*
5154	2.314	-0.0633*
5086	2.831	-0.0072

*Unreliable because of poor statistics.

performed at a mill where many alloys can be tested over a long period of time using resistivity measurement devices that have been optimized for use in the mill environment and are well calibrated.

Most of the large uncertainty in $\Delta\rho$ as measured by the entrance eddy-current probe can be traced to the uncertainty in the temperature measurement by the contact thermocouple on the hot slab by the following arguments. The value of $\Delta\rho$ associated with a particular alloy was calculated from

$$\Delta\rho = \rho_c(T) - \rho_a(T), \quad (16)$$

where $\rho_c(T)$ is the resistivity of the hot slab deduced from impedance measurements with eq (15) and $\rho_a(T)$ is the resistivity of pure aluminum at the temperature, T , where T is the temperature measured by the contact thermocouple. The uncertainty in $\Delta\rho$ associated with this procedure is

$$\delta\Delta\rho = \{[\delta\rho_c]^2 + [(\partial\rho/\partial T)\delta T]^2\}^{1/2}, \quad (17)$$

where $\delta\rho_c$ is the uncertainty in measuring the resistivity with the high temperature probe and $(\partial\rho/\partial T)\delta T$ is the uncertainty in the resistivity value caused by an uncertainty in the temperature measurement of magnitude $\pm\delta T$. The quantity $\delta\rho_c$ was estimated from repeated measurements of the resistivity of slabs with resistivities comparable to those encountered at high temperature. Thick samples of 6061 aluminum ($\rho = 3.6 \mu\Omega\cdot\text{cm}$) and of brass ($\rho = 6.2 \mu\Omega\cdot\text{cm}$) were tested with the high-temperature probe operating at room temperature and it was found that the 3σ

uncertainty for these alloys was $\delta\rho_c = 0.04 \mu\Omega\cdot\text{cm}$. For high-temperature aluminum with an average resistivity of $9 \mu\Omega\cdot\text{cm}$, this uncertainty in resistivity would be $0.073 \mu\Omega\cdot\text{cm}$.

Estimation of this error in the temperature, δT , was the purpose of a concentrated effort by personnel from another aluminum manufacturer, two manufacturers of infra-red sensors and NIST [2] who all used commercial thermocouples held against the hot slabs being processed at the mill at the same time the eddy-current tests were being performed. Their results were reported to the Aluminum Association in special reports in February and April of 1996 and gave a standard deviation in the temperature measurement of between $\pm 2^\circ\text{C}$ and $\pm 4^\circ\text{C}$ depending on the how the thermocouple was mechanically supported and how the data were analyzed. Our own measurements presented in Appendix A made in the fall of 1996 using a contact thermocouple on the end of a hand-held wand, indicated a similar result of $\pm 3^\circ\text{C}$ for the standard deviation in the measurement of the temperature of the hot slab. Taking $\pm 3^\circ\text{C}$ as representative of the temperature uncertainty and multiplying by 3 to get the 3σ uncertainty yields $\delta T(3\sigma) = 9^\circ\text{C}$ for the temperature uncertainty. This translates to a resistivity uncertainty of $(\partial\rho_a/\partial T)\delta T = \pm 0.117 \mu\Omega\cdot\text{cm}$ (3σ) through the use of the inverse of eq (6). Combining the main sources of uncertainty in eq (10) determines the error in the alloy contribution to be

$$\delta\Delta\rho = 77 [(0.073)^2 + (0.117)^2]^{1/2} = 0.14 \mu\Omega\cdot\text{cm}(3\sigma). \quad (18)$$

This value is completely consistent with the scatter observed in the data from the entry eddy-current probe on the 59 coils tested with the contact thermocouple and displayed in Figure 4(a). Thus, it can be concluded that the uncertainty displayed in Figure 4(a) arises mainly from the temperature uncertainty with a secondary portion from the impedance measurement.

3. TEMPERATURE ERROR FOR THE TOTAL SYSTEM

The complete eddy-current thermometer requires measurements by a noncontacting probe at the exit end of the hot mill and a contacting probe at the entrance to the hot mill. Thus, the uncertainty in the exit temperature is a combination of the uncertainties from each probe. Equation (9) gives this combination in terms of the uncertainty, $\delta\rho(T)$, in the resistivity measurement at the exit end, and the uncertainty, $\delta\Delta\rho$, in the alloy resistivity. The latter error is actually made up of two terms, the uncertainty from the impedance measurement, $\delta\rho_c$, and the uncertainty, $(\partial\rho/\partial T)\delta T$, from the thermocouple measurement of the temperature. Thus, the temperature uncertainty for the total system can be written

$$\delta T = 77 \{[\delta\rho(T)]^2 + [\delta\rho_c]^2 + [\partial\rho/\partial T]\delta T\}^{1/2}. \quad (19)$$

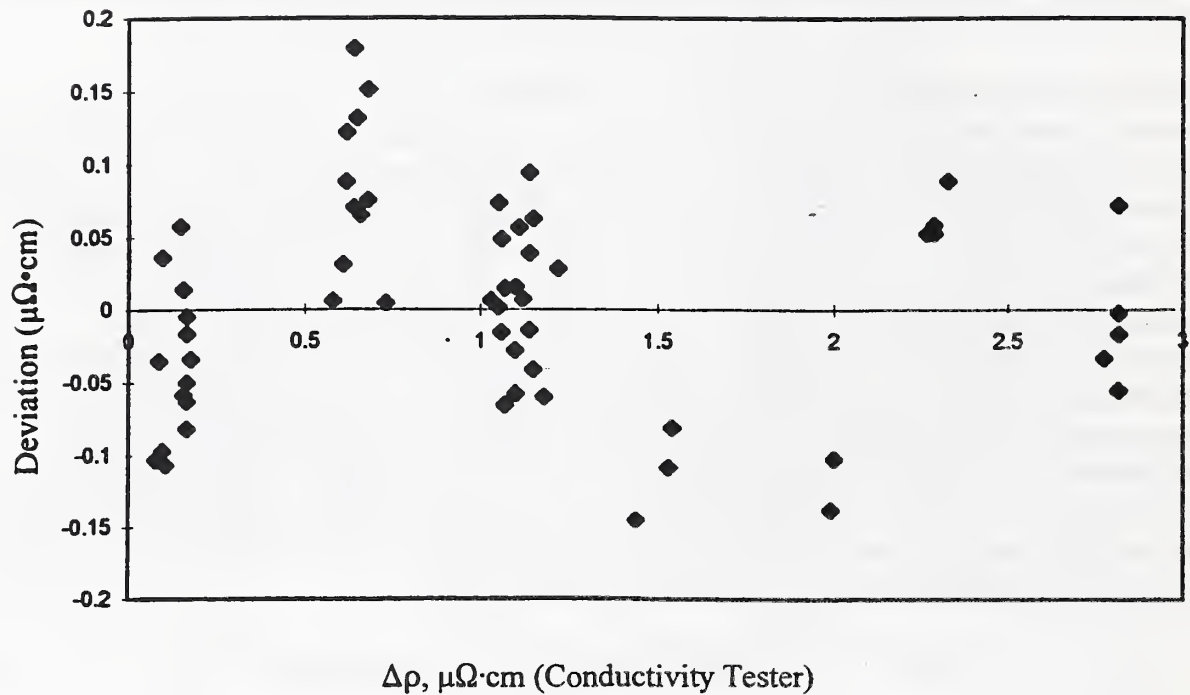


Figure 4(a). Deviation of individual $\Delta\rho$ measurements made by the entrance eddy-current probe from the $\Delta\rho$ measurements made by the commercial conductivity tester as a function of the latter.

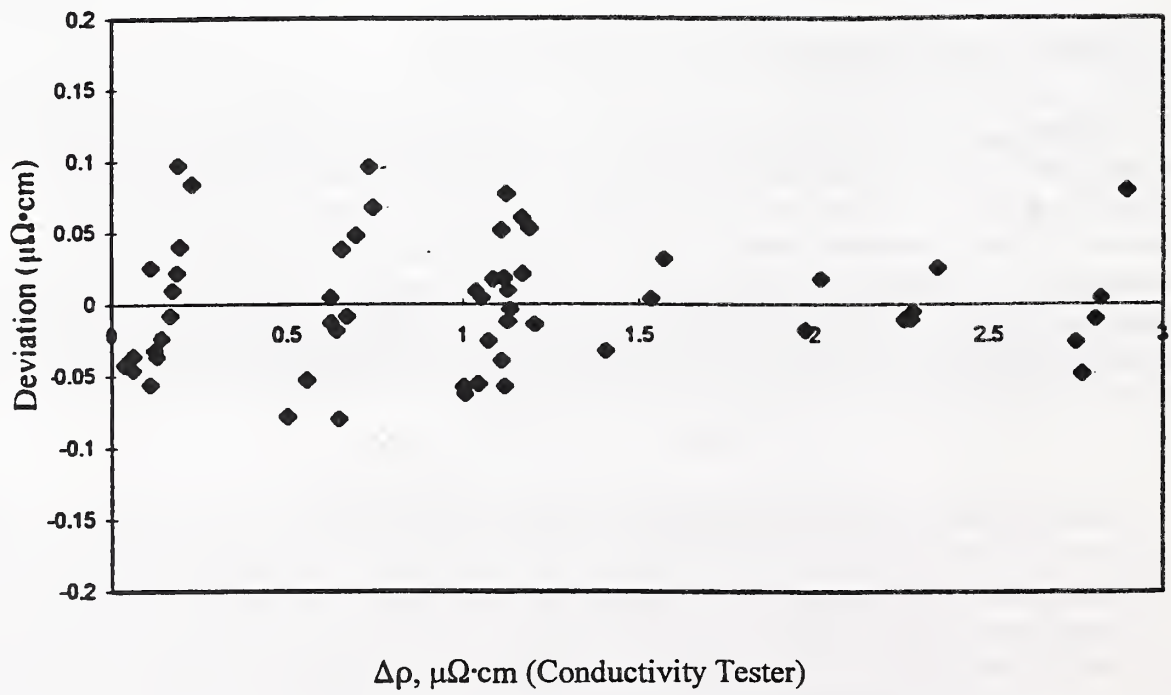


Figure 4(b). Same as Fig. 4(a) after addition of corrections to Matthiessen's rule for each alloy.

In the previous sections, each of these terms was discussed separately. For the conditions at the actual rolling mill, the three terms were:

$$\begin{aligned} \delta\rho &= 0.6\% \text{ of } 9 \mu\Omega\cdot\text{cm} && = \pm 0.054 \mu\Omega\cdot\text{cm} \\ \delta\rho_c &= \text{error in the entrance probe impedance measurement} && = \pm 0.073 \mu\Omega\cdot\text{cm} \\ (\partial\rho/\partial T)\delta T &= \text{standard deviation of } \pm 3^\circ\text{C} \text{ in the contact thermocouple} && = \pm 0.117 \mu\Omega\cdot\text{cm}, \end{aligned}$$

which, when combined in eq (19), yield the total 3σ uncertainty in the system exit temperature of $\delta T = \pm 11^\circ\text{C}$.

More recent tests of the variability in contact temperature measurements appear to indicate that an uncertainty of $\pm 1^\circ\text{C}$ is reasonable. This would lower the last term in the list above from $\pm 0.117 \mu\Omega\cdot\text{cm}$ to $\pm 0.04 \mu\Omega\cdot\text{cm}$ and the total 3σ temperature uncertainty to $\pm 8^\circ\text{C}$.

To put these results in context and to point out where improvements would be most effective, a table showing the results of changing each of the three sources of uncertainty was prepared. This table is shown as Table 4 and presents the temperature uncertainty to be expected under a variety of conditions.

Cases 1 and 2 describe the current situation with a very conservative choice for the uncertainties due to the temperature measurement. Case 3 ($\pm 9^\circ\text{C}$) would be obtainable with a modest

Table 4. Consequences of various improvements in the measurement technique.

Case	Primary error source or suggested improvement	$\delta\rho$	$\delta\rho_c$ $\mu\Omega\cdot\text{cm}$	$(\delta\rho/\delta T)\delta T$ $\mu\Omega\cdot\text{cm}$	$\delta T(3\sigma)$ $^\circ\text{C}$
1.	Look-up table for $\Delta\rho$	0.054	0.14 to 0.19		± 11 to 14
2.	$\pm 3^\circ\text{C}$ thermocouple uncertainty (1σ)	0.054	0.073	0.117	+11
3.	$\pm 2^\circ\text{C}$ thermocouple uncertainty (1σ)	0.054	0.073	0.078	± 9
4.	ρ measurements to $1\sigma = 0.2\%$; T to $\pm 2^\circ\text{C}$ (1σ)	0.054	0.054	0.078	± 8.3
5.	Correction for matthiessen's rule (Table 3)	0.054		0.09	± 8
6.	ρ measurements to $1\sigma = 0.2\%$; T to $\pm 1^\circ\text{C}$ (1σ)	0.054	0.054	0.038	± 6.5
7.	Optimized ρ measurements to $1\sigma = 0.1\%$; T to $\pm 1^\circ\text{C}$ (1σ)	0.027	0.027	0.038	± 4.2

improvement in the application of the contact thermocouple to the hot slab. Cases 4 and 5 ($\pm 8^\circ\text{C}$) would be achieved by reducing the uncertainty in the measurement of the entrance probe impedance to the same accuracy as attained at the exit end plus a look-up table correction to Matthiessen's rule. Case 6 ($\pm 6.5^\circ\text{C}$) appears possible if the uncertainty in the temperature measurement of the hot slab can be reduced to $\pm 1^\circ\text{C}$ (1σ).

4. CONCLUSIONS

1. By using eddy-current principles, we can measure the resistivity of aluminum alloy sheet metal as it leaves the final reduction stand of an operating hot mill without any physical contact with the sheet. The resistivity measurements are not seriously influenced by the speed of the sheet, its location compared with the pass line or the presence of lubricants and cooling fluids on the sheet. A separate measurement of the sheet thickness by an adjacent X-ray thickness gage is required to convert the electrical quantities measured into an absolute value for the resistivity.

2. By defining the resistivity of any alloy as the simple sum of the temperature dependent resistivity of pure aluminum plus a temperature-independent term characteristic of the particular alloy, we can convert a measured resistivity value into a temperature and thus provide a noncontacting thermometer whose output is a continuous measurement of the exit temperature of the sheet just before coiling.

3. To make the actual conversion to temperature, a correction factor for the specific alloy being processed must be introduced. If this correction factor is taken from a look-up table for the nominal composition of the alloy, the 3σ uncertainty in the exit temperature of the sheet can be as much as $\pm 14^\circ\text{C}$. If a contacting eddy-current probe is added to the entrance end of the hot mill where a contact thermocouple measures the temperature of the alloy slab entering the hot mill, the alloy correction factor can be directly measured and the 3σ uncertainty can be reduced to about $\pm 8^\circ\text{C}$.

4. If modern laboratory techniques are used to better calibrate the resistivity of pure aluminum at high temperature and establish the alloy contribution to the resistivity, the primary source of uncertainty in the exit temperature appears to be the uncertainty arising from the contact thermocouple operating on the hot slab to determine the alloy correction factor. If the 3σ uncertainty in the contacting thermometer at the entrance end could be reduced from $\pm 6^\circ\text{C}$ to $\pm 3^\circ\text{C}$, the 3σ uncertainty in the exit temperature could approach $\pm 6^\circ\text{C}$. If the resistivity measurements could be reduced to $\pm 0.1\%$ (1σ) by optimizing commercial instrumentation currently available, the 3σ uncertainty in the exit temperature could be reduced to near $\pm 4^\circ\text{C}$.

This report is the culmination of many years of effort centered mainly at the National Institute of Standards and Technology (NIST) in Gaithersburg, Maryland. As a result, it represents the cumulative effort of many different people. In the early days, M.L. Mester made major

contributions as a NIST Research Associate supported by the Aluminum Association. Adin Stern, a NIST Visiting Scientist from Israel, made many precise measurements of resistivity on commercial alloys to establish the validity of Matthiessen's rule and to place bounds on the ultimate accuracy to be expected by the eddy-current approach. Chris Burnett and Richard Musgrove of Data Measurements Corporation provided valuable support by building and installing the eddy-current coils for the exit probe at the Alumax Mill in Lancaster, PA. Denzil Mathews of the NIST Metallurgy Division was indispensable during the collection of on-line data at the mill during the unusually hot summer of 1995.

The work could never have been accomplished without the cooperation of the Production Staff of the Mill Products Division of Alumax Corporation and the support and guidance of the Staff Metallurgist, Charlie Kahler. The Task Force on Noncontact Temperature Sensing of the Aluminum Association deserve special thanks for their support and guidance during this program. Jerry Dassel of Commonwealth Aluminum and Mike Johannes made many valuable contributions during the preparation of this report.

5. REFERENCES

- [1] Kahn, A.H.; Phillips, L.C.; Stern, A. "Electromagnetic Monitoring of Metals Processing," Materials Engineering Conference VI, Haifa, Israel: Freund Publishing House; March 1993.
- [2] Anderson, D.; Kirby, P.; Nawfel, P. Pyrometer Capability Tests, Special Report to the Non-contact Temperature Sensor Measurement Task Group of the Aluminum Association, S.G. Epstein, Staff Executive, 900 19th St., NW, Washington, DC 20006, 1996.
- [3] Fickett, F.R. Aluminum 1. A Review of Resistive Mechanisms in Aluminum, Cryogenics, Vol. 11, p 349, 1971 and "Electrical Properties," Materials at Low Temperatures, Metals Park, OH: American Society for Metals; 1983.
- [4] Aluminum Properties and Physical Metallurgy, John E. Hatch, ed. Metals Park, OH: American Society for Metals, 1984. 9,11.
- [5] Armour Research Foundation, Handbook of Thermophysical Properties of Solid Materials, MacMillan Co.; 1961. 53.
- [6] Handbook of Chemistry and Physics," CRC Press, 74th Edition, 1993.
- [7] T.E. Pochapsky, Acta Met., Vol. 1, 1953, 747.

APPENDIX A - Data collected at the Alumax Mill in August 1996.

1 Sept.	2 Index	3 Alloy	4 $\Delta\rho$	5 T (°C)	6 Phase	7 Magnitude	8 eq 15	9 ρ (T)
29	0	5152	2.78	458	1.346322	0.438574	10.5484052	10.5816132
29	1	5152	2.82	457	1.343482	0.43558	10.5532103	10.6085506
29	2	5152	2.82	452	1.341568	0.434376	10.6153994	10.5433246
29	4	5152	2.82	457	1.343333	0.436148	10.6059871	10.6085506
29	5	5152	2.82	459	1.34589	0.439066	10.6177676	10.6346817
29	6	1100	0.16	399	1.364663	0.411325	7.14278922	7.20087491
29	7	1100	0.17	398	1.364126	0.411445	7.19340024	7.19815564
29	9	1100	0.15	397	1.363651	0.411341	7.22294498	7.16544219
29	10	1100	0.17	401	1.363925	0.410957	7.17373958	7.23633091
29	11	1100	0.17	399	1.363947	0.411267	7.19447866	7.21087491
29	19	1145	0.1	469	1.359974	0.417397	7.94866824	8.04568651
29	20	1145	0.1	459	1.35994	0.417392	7.95096008	7.91468171
29	21	1145	0.11	472	1.359081	0.416982	7.98831322	8.09510144
29	22	1145	0.08	473	1.35982	0.4176	7.9753948	8.07825139
29	25	1145	0.09	463	1.360381	0.417466	7.92189618	7.95701379
29	26	5052	1.99	456	1.34895	0.428697	9.62777368	9.76549376
29	27	5052	2	454	1.349784	0.429863	9.64713668	9.74939756
30	41	5052	1.44	454	1.35318	0.425201	9.04432964	9.18939756
30	43	3105	1.14	458	1.353397	0.425325	9.03637318	8.94161324
30	44	3105	1.15	456	1.353187	0.42444	8.98865638	8.92549376
30	46	3105	1.22	452	1.351918	0.422831	8.97115856	8.94332464
30	48	3105	1.14	453	1.353706	0.423981	8.91489328	8.87635819
30	53	5005	0.62	446	1.356138	0.418856	8.35379636	8.26524556
30	54	5005	0.66	452	1.355413	0.41939	8.44907282	8.38332464
30	59	5005	0.64	450	1.356882	0.420412	8.40843636	8.337275
30	61	5005	0.64	441	1.355709	0.419031	8.3999611	8.22033971
30	62	5005	0.62	451	1.35599	0.420061	8.45263944	8.33029691
30	64	5005	0.68	454	1.355364	0.420114	8.50534432	8.42939756
30	65	5005	0.65	453	1.355619	0.420571	8.5185441	8.38635819
30	66	5005	0.61	453	1.356301	0.419361	8.37765478	8.34635819
30	68	5005	0.73	453	1.35563	0.419922	8.47067188	8.46635819
30	69	5005	0.68	451	1.355624	0.420896	8.5416968	8.39029691
30	72	5005	0.58	458	1.357648	0.420948	8.38747024	8.38161324
30	74	3105	1.06	453	1.35641	0.425044	8.78082276	8.79635819
30	75	3005	1.53	486	1.35214	0.431625	9.5908666	9.69973036
30	80	3005	1.54	489	1.359548	0.44068	9.66854232	9.74944211
31	82	5154	2.33	472	1.337712	0.427305	10.4041755	10.3151014
31	83	5154	2.27	473	1.341292	0.430012	10.3208158	10.2682514
31	84	5154	2.29	473	1.34104	0.430097	10.3466443	10.2882514
31	85	5154	2.29	473	1.344605	0.433865	10.3413143	10.2882514
31	86	3003	1.05	440	1.353003	0.420139	8.69145498	8.617376
31	88	3003	1.07	440	1.354785	0.420412	8.57212818	8.637376
31	89	3003	1.03	433	1.354453	0.41924	8.51314442	8.50679299
31	90	3003	1.06	433	1.354347	0.420124	8.58545574	8.53679299
31	91	1100	0.17	383	1.366434	0.410245	6.92630976	7.00806499
31	92	1100	0.17	384	1.365761	0.410135	6.97087574	7.02069696
31	93	1100	0.18	386	1.365998	0.411096	7.02199036	7.05597836
31	94	1100	0.16	382	1.366752	0.411596	6.99935312	6.98543884
31	96	3003	1.1	434	1.356809	0.422037	8.53184974	8.58971596
31	97	3003	1.1	436	1.356498	0.422467	8.5872756	8.61557936
31	98?		1.18	434	1.3561	0.422347	8.60965068	8.66971596
31	99	3003	1.12	433	1.355306	0.421411	8.60382648	8.59679299
31	100	3003	1.07	436	1.355818	0.421914	8.60029708	8.58557936
31	101	3003	1.11	426	1.357367	0.42294	8.55370558	8.49649516
31	102	3003	1.1	431	1.355964	0.4216	8.56615416	8.55096451
31	103	3003	1.15	432	1.356621	0.422392	8.57224122	8.61387584
31	104	3003	1.09	423	1.355078	0.421181	8.60496296	8.43788339
31	105	3003	1.14	434	1.356093	0.422415	8.61512302	8.62971596
31	106	3003	1.05	429	1.355725	0.420112	8.47701978	8.47515931

APPENDIX B - Resistivity of Aluminum

Literature references 5, 6 and 7 give values for the resistivity of pure aluminum as a function of temperature above room temperature. Table 1B lists these values for comparison and the graph shows how these values differ from eq (2).

Table 2B lists values for the alloy contribution, $\Delta\rho$, for various commercial alloys heat treated in different ways. (Data taken from Ref. 3.)

Table 1B. Literature values for the resistivity of pure aluminum.

Temp. °C	Ref. 5 $\mu\Omega\cdot\text{cm}$	Ref. 6 $\mu\Omega\cdot\text{cm}$	Ref. 7 $\mu\Omega\cdot\text{cm}$	Eq.2 $\mu\Omega\cdot\text{cm}$
0		2.417	2.428	2.428
27	2.66	2.73		2.71
100			3.516	3.5
127	3.82	3.87		3.8
200			4.64	4.62
227	5	4.99		4.94
300			5.82	5.81
327	6.18	6.13		6.14
400			7.08	7.05
427	7.45	7.35		7.4
500			8.38	8.36
527	8.83	8.7		8.72
550			9.08	9.03
600			9.8	9.73
625			10.19	10.06

Table 2B. Literature values for the alloy contribution to the resistivity of aluminum (Ref.3)

Alloy	Temperature	$\Delta\rho \mu\Omega\cdot\text{cm}$
1100	0	0.082
2014	T651	1.531
2024	0	0.583
2024	T4	1.742
2024	T6	1.337
2024	T86	1.578
5083	H113	3.07
5083	0	3.03
6061	T6	1.381
7039	T61	1.738
7039	0	2.12
7075	T73	1.092
7075	T6	2.76

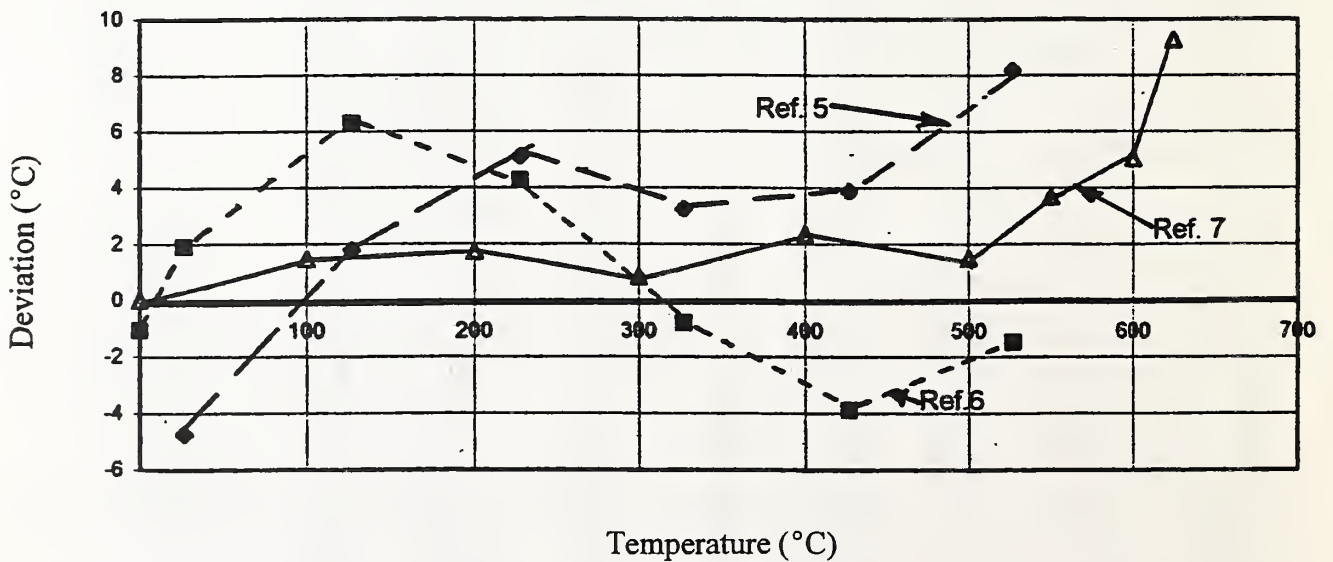


Figure B-1. Difference between eq (2) and Refs. 5, 6, and 7 expressed as degrees Celsius.

